Kinetic Mechanism of Blebbistatin Inhibition of Nonmuscle Myosin IIB†

Bhagavathi Ramamurthy,‡ Christopher M. Yengo,‡,§ Aaron F. Straight,⊥,|| Timothy J. Mitchison,⊥ and H. Lee Sweeney*,‡

Department of Physiology, University of Pennsylvania School of Medicine, 3700 Hamilton Walk, Philadelphia, Pennsylvania 19104, and Department of Cell Biology and Institute of Chemistry and Cell Biology, Harvard Medical School, 250 Longwood Avenue, Boston, Massachusetts 02115

Received May 13, 2004; Revised Manuscript Received August 30, 2004

ABSTRACT: We examined the effect of blebbistatin on the kinetic properties of nonmuscle myosin IIB subfragment 1 (NMIIB S1). Blebbistatin is a small molecule that affects cell blebbing during the process of cell division, which has been shown to decrease the myosin ATPase activity of a number of myosins [Straight et al. (2003) *Science 299*, 1743−1747]. The steady-state actin-activated ATPase activity of NMIIB S1 was decreased ~90% at 40 μM actin in the presence of blebbistatin. Stopped-flow techniques were employed to elucidate the effect of blebbistatin on the various steps of the NMIIB S1 cross-bridge cycle. Blebbistatin did not affect ATP binding and hydrolysis. Binding to actin in the presence of ADP ($0.57 \pm 0.08\ \mu M^{-1}\ s^{-1}$) was reduced slightly in the presence of blebbistatin ($0.38 \pm 0.03\ \mu M^{-1}\ s^{-1}$), while mantADP dissociation from acto-NMIIB S1 was reduced (~30%). P_i release was blocked in the presence of blebbistatin. Accordingly, the apparent affinity of NMIIB S1 for actin in the presence of ATP was greatly reduced. Based on the above data, we surmise that blebbistatin inhibits the ATPase activity of NMIIB S1 primarily by blocking entry into the strong binding state; secondarily, it reduces the rate of ADP release. These effects are likely mediated by binding of blebbistatin within the myosin cleft that progressively closes in forming the acto-myosin rigor state.

Myosin II isoforms are molecular motors expressed widely in almost all eukaryotic cell types. Myosins are ATPase enzymes that are activated by actin, and this activation increases the ATPase activity multifold to different extents in different isoforms. All class II myosins are hexameric with each of the two heavy chains binding essential and regulatory light chains. The N-terminal motor domain of the heavy chain contains the nucleotide and actin binding sites and confers ATPase activity. Light chains are present at the neck region of the heavy chain. Specific isoforms of the muscle myosins are present in specific muscles, whereas nonmuscle myosin isoforms are ubiquitously expressed in several cell types.

Nonmuscle myosin IIB comprises approximately 70% of the myosin II found in the central nervous system and 100% of cardiac nonmuscle myosin II. Nonmuscle myosin IIB is a well-studied protein, and the kinetic characteristics are documented (*1*, *2*). This myosin shares a number of features with processive unconventional myosins. These features include high ADP affinity, high duty ratio, and slow ADP release (*1*, *2*).

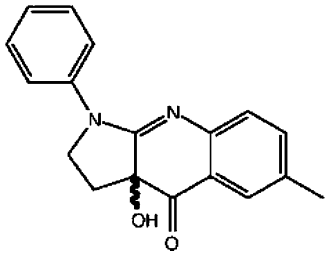

FIGURE 1: Structure of (±)-blebbistatin (from ref *5*).

Small molecule inhibition of myosins has been studied with various other inhibitors in an attempt to find either a universal or a class-specific myosin inhibitor. Inhibitors such as 2,3-butanedione monoxime (BDM) (*3*) and *N*-benzyl-*p*-toluene sulfonamide (BTS) (*4*) have been shown to differentially inhibit specific myosins. Blebbistatin (1-phenyl-2-pyrrolidinone derivative, Figure 1) is a small molecule that inhibits steady-state actin-activated ATPase activity of NMIIB[1] heavy mero myosin (HMM) (*5*). It is also shown to inhibit myosin II and thereby inhibit pancreatic adenocarcinoma cellular invasiveness in the pancreas (*6*). While blebbistatin has been shown to affect function of myosin II in many cell types, the kinetic mechanisms of the inhibition of myosins by blebbistatin are yet to be studied. In this study, we have systematically examined the effect of blebbistatin

† This study was supported by a grant from NIH, No. RO1 AR35661 to H.L.S.

* Corresponding author. Mailing address: Department of Physiology, University of Pennsylvania School of Medicine, 3700 Hamilton Walk, B400 Richards Building, Philadelphia, PA 19104-6085. Phone: 215-898-8726. Fax: 215-573-2273. E-mail: lsweeney@mail.med.upenn.edu.

‡ University of Pennsylvania School of Medicine.

§ Current address: Department of Biology, University of North Carolina at Charlotte, 9201 University City Blvd., Charlotte, NC 28223.

⊥ Harvard Medical School.

|| Current Address: Department of Biochemistry, Stanford University School of Medicine, B409A, 279 Campus Drive, Stanford, CA 94305-5307

[1] Abbreviations: NMIIB S1, nonmuscle myosin IIB subfragment 1; MDCC−PBP, *N*-[2-(1-maleimidyl)ethyl]-7-(diethylamino)coumarin-3-carboxamide-labeled phosphate binding protein; ATP, adenosine triphosphate; ADP, adenosine diphosphate; P_i, inorganic phosphate; DMSO, dimethyl sulfoxide.

10.1021/bi0490284 CCC: $27.50
Published on Web 10/28/2004

on the kinetics of the ATPase cycle of nonmuscle myosin IIB subfragment 1.

MATERIALS AND METHODS

Recombinant Myosin IIB Expression and Purification. Single-headed S1-like myosin IIB (henceforth referred to in the manuscript as NMIIB S1) constructs were created from truncation of chicken nonmuscle IIB heavy chain cDNA at Leu845 (B1 isoform of loop1 with no loop 2 insertion). A FLAG tag (encoding DYKDDDDK) was inserted at the C-terminus to facilitate purification. Both essential light chain (ELC) and regulatory light chain (RLC) binding sites (IQ motifs) were present in the recombinant heavy chain protein. Expression of the recombinant myosin IIB S1 was accomplished via infection of SF9 insect cells with a baculovirus expression vector capable of driving high-level expression of foreign proteins. The SF9 cells were co-infected with recombinant virus expressing the myosin IIB heavy chain and recombinant viruses for the nonmuscle ELC and RLC. Myosin was purified as described (*7*).

Actin Purification and Reagents. Actin was purified from rabbit skeletal muscle using acetone powder (*8*), gel filtered, and labeled with pyrenyl iodoacetamide (Molecular Probes) as described (*9*). All reagents were of the highest purity commercially available. ATP was prepared fresh from dry powder (Roche Molecular Biochemicals, 99.7% pure by HPLC, data not shown).

Blebbistatin was provided by Drs. Aaron F. Straight and T. J. Mitchison (Harvard Medical School, Boston, MA). An enantiomeric mixture of blebbistatin dissolved in DMSO was used. All dilutions of blebbistatin in the experiments were made in DMSO keeping a maximum of 5% DMSO in assay mixtures to minimize deleterious effects on proteins. The compound was stored at −80 °C in the dark until use to prevent photoinactivation. NMIIB S1 was incubated with blebbistatin in all experiments at 5% DMSO prior to mixing with the required reactants to obtain readings in the stopped flow system.

All assays were performed in low-salt buffer (20 mM MOPS, 20 mM KCl, 5 mM $MgCl_2$, 1 mM EGTA, 1 mM DTT, pH 7.0, 25 °C).

Actin-Activated ATPase Activity. Steady-state ATP hydrolysis by NMIIB S1 (200 nM) was measured in the presence (0−100 μM) and absence of actin using the NADH-linked assay (*10*) with a final MgATP concentration of 1 mM.

Kinetics and Modeling. Transient kinetic measurements were performed in an Applied Photophysics (Surrey, U.K.) SX 18MV stopped flow apparatus, which has a dead time of 1.2 ms. Tryptophan fluorescence was measured with an excitation wavelength of 295 nm, and emission was measured using a 320 nm long-pass filter (Oriel Corp., Stratford, CT). Pyrene actin and mant-labeled nucleotides were excited at 365 nm, and the fluorescence emission was measured using a 400 nm long-pass filter (Oriel Corp., Stratford, CT). Chemical quench experiments were performed to determine the amplitude of the ADP−P_i burst of NMIIB S1, and activated charcoal was used to measure $^{32}P_i$ generated from the hydrolysis of [γ-^{32}P]ATP as described (*11*), after manual mixing. Transient P_i release was measured by using the coupled assay system containing the bacterial phosphate binding protein (PBP) labeled covalently with *N*-[2-(1-maleimidyl)ethyl]-7-(diethylamino)coumarin-3-carboxamide (MDCC−PBP) as described (*12*), by exciting at 425 nm and measuring emission using a 455 nm long-pass filter. Background P_i was removed by incubating the stopped flow apparatus and all solutions with 7-methyl-guanosine (0.1 mM) and purine nucleoside phosphorylase (0.02 units/mL).

Nonlinear least-squares fitting of the data was done with software provided with the instrument or Kaleidagraph (Synergy Software, Reading, PA). All values are presented with a standard error of the fit and as the mean ± SD for multiple trials.

Scheme 1[a]

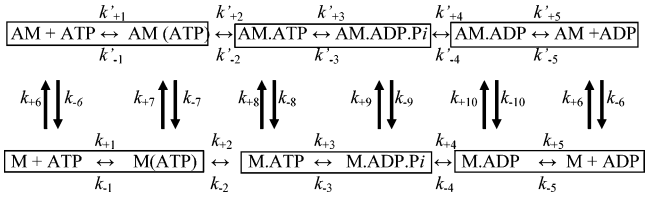

[a] A is actin; M is myosin; P_i is inorganic phosphate.

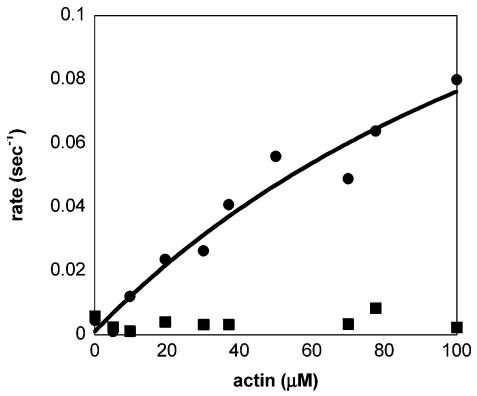

FIGURE 2: Effect of 100 μM (±)-blebbistatin on the steady-state actin-activated MgATPase activity of nonmuscle myosin IIB. Actin-activated ATPase activity of NMIIB S1 (●) is fitted to a hyperbolic Michaelis−Menten equation with a V_{max} of 0.2 ± 0.11 s^{-1} and a K_{ATPase} of 176 ± 152 μM^{-1}. ATPase activity is inhibited (>90%) by blebbistatin. Data from the blebbistatin-treated NMIIB S1 samples (■) could not be fitted to the Michaelis−Menten equation.

RESULTS

We examined the effect of blebbistatin on the kinetics of each of the steps in the mechanochemical cycle of NMIIB S1. The framework used in this study is as described in Scheme 1. DMSO was used to solubilize blebbistatin. Independent measurements using DMSO as a control to test its effect on NMIIB S1 were performed for all experiments. DMSO did not alter any of the kinetic steps except ATP-induced dissociation from actin and ADP release. All concentrations mentioned in the stopped flow experiments are initial concentrations unless otherwise stated.

Steady-State ATPase Activity. Actin-activated ATPase activity of NMIIB S1 with and without blebbistatin was measured using an NADH-coupled assay (Figure 2). The steady-state turnover of ATP by NMIIB S1 is very slow in the absence of actin (0.012 ± 0.0007 s^{-1}). Actin activates the ATPase activity ~20-fold (V_{max} = 0.20 ± 0.11 s^{-1}). Blebbistatin inhibits actin-activated MgATPase activity by >90%.

Table 1: Kinetic Parameters of Blebbistatin Effect on NMIIB S1

parameter	signal	unit	−bleb	+bleb
basal ATPase	NADH-coupled assay	s^{-1}	0.012 ± 0.007	0.007 ± 0.0001
Actin-Activated ATPase Activity				
V_{max}	NADH-coupled assay	s^{-1}	0.20 ± 0.1	
K_{ATPase}	NADH-coupled assay	μM	176 ± 152	
ATP Binding				
K_1k_{+2}	tryptophan	s^{-1}	0.48 ± 0.09	
K_1k_{+2}	mant	μM^{-1} s^{-1}	0.74 ± 0.02	0.72 ± 0.03
$K'_1k'_{+2}$	mant	μM^{-1} s^{-1}	0.62 ± 0.04	0.58 ± 0.03
k'_{+2}	pyrene	s^{-1}	474 ± 10	291 ± 37
K'_1	pyrene	μM	229 ± 15	201 ± 92
$K'_1k'_{+2}$[a]	pyrene	μM^{-1} s^{-1}	0.86 ± 0.10	0.44 ± 0.02
ATP Hydrolysis				
P_i burst	chemical quench		0.30 ± 0.05	0.33 ± 0.06
K_3	chemical quench		0.44 ± 0.06	0.5 ± 0.07
Actin Binding to S1−ADP				
k_{+10}	pyrene	μM^{-1} s^{-1}	0.57 ± 0.08	0.38 ± 0.07
P_i Release				
k'_{+4}	MDCC−PBP	s^{-1}	0.03 ± 0.003	
ADP Dissociation				
k_{+5}	mant	s^{-1}	1.8 ±.028	1.3 ± 0.098[b]
k'_{+5}	mant	s^{-1}	1.8 ± 0.22	0.9 ± 0.10[c]

[a] K'_1 deduced from initial slope of the ATP-induced dissociation of pyrene−actin curve. [b] DMSO treatment contributed a drop to 1.5 ± 0.08 s^{-1}. [c] DMSO treatment contributed a drop to 1.4 ± 0.28 s^{-1}.

Photoinactivation of Blebbistatin. Blebbistatin is a photosensitive compound. NMIIB S1 and 30 μM actin incubated with 200 μM blebbistatin was exposed for 5 s to 295 and 365 nm and for 1 s to 425 nm wavelengths of light before reacting with ATP to measure actin-activated ATPase in an NADH-coupled assay. Samples containing blebbistatin exposed to 295 nm light for 5 s did not inhibit actin-activated ATPase activity of NMIIB S1 (0.27 ± 0.007 s^{-1}). However, exposure of blebbistatin incubated acto-NMIIB S1 to 365 nm light for 5 s inhibited ATPase activity to 0.03 ± 0.01 s^{-1} reflecting the active nature of the compound. Exposure of acto-NMIIB S1 incubated with blebbistatin to 425 nm light for 1 s did not inhibit ATPase activity; rather an increase in ATPase activity (0.36 ± 0.01 s^{-1}) compared to unexposed controls (0.17 ± 0.0007 s^{-1}) was observed.

ATP-Induced Dissociation of Acto-NMIIB S1. Rapid mixing of MgATP with the pyrene−acto-NMIIB S1 complex causes an increase in fluorescence levels of pyrene−actin, which reflects the ATP-induced population of the weakly bound states of myosin. Pyrene−acto-NMIIB S1 (2.5 μM) was mixed with varying amounts of ATP (0−1000 μM) in the stopped flow apparatus. A plot of the observed rate constant of the increase in fluorescence as a function of MgATP concentration was hyperbolic and saturated at 474 ± 10 s^{-1} and reached half-maximum at 229 ± 15 μM ATP (Table 1). Blebbistatin (100 μM) reduced the maximum rate of ATP-induced dissociation (k'_{+2} = 291 ± 37 s^{-1}) and the ATP concentration at which half-maximal saturation occurs to 201 ± 92 μM^{-1} s^{-1}. The apparent second-order association rate constant for MgATP binding to pyrene−acto-NMIIB S1 ($K'_1k'_{+2}$) obtained from the initial slope of the plot at low ATP concentration was 0.86 ± 0.01 μM^{-1} s^{-1}, and with blebbistatin treatment, it was 0.44 ± 0.02 μM^{-1} s^{-1} (Table 1). Unfortunately, the levels of DMSO needed to solubilize blebbistatin had a significant effect on the maximum rate of ATP-induced dissociation of acto-NMIIB S1 (k_{+2} = 377 ± 20 s^{-1}). Therefore, it was not possible to determine whether blebbistatin alone had any effect on k_{+2}.

mantATP Binding and ATP Hydrolysis. Since the results of the ATP-induced dissociation were difficult to interpret, we examined ATP binding with mantATP. Binding of mantATP to NMIIB S1 in the presence and absence of actin results in an increase of fluorescent signal of the mant nucleotide as in many other myosin isoforms. This reaction was modeled according to Scheme 1, in which ATP binding is a two-step process, a rapid equilibrium collision complex (K_1) followed by an isomerization (K_2) to form the myosin−ATP complex. NMIIB S1 (2 μM) was mixed with varying amounts of mantATP (0−30 μM) and gave a K_1k_{+2} of 0.74 ± 0.02 μM^{-1} s^{-1}. Blebbistatin (100 μM) was incubated with NMIIB S1, and this treatment did not change the rate constant of mantATP binding (0.72 ± 0.03 s^{-1}) (Figure 3A). Dependence of mantATP binding to acto-NMIIB S1 (5 μM actin) gave an apparent second-order rate constant of 0.62 ± 0.04 s^{-1}. Blebbistatin (100 μM) treatment of acto-NMIIB S1 showed an apparent second-order rate constant of 0.56 ± 0.03 s^{-1} (Figure 3B; Table 1).

Based on earlier work on NMIIB S1 (*1*, *2*), which measured the tryptophan fluorescence enhancement upon ATP binding, a hyperbolic increase in the rate constant as a function of ATP concentration was observed with a saturation rate of 16.5 ± 0.2 (*2*) and 16.7 ± 1.1 s^{-1} (*1*). Thus at high ATP concentrations, the rate of fluorescence enhancement is limited by the ATP hydrolysis step, and its maximal rate reports the rate of ATP hydrolysis ($k_{+3} + k_{-3}$). At low ATP concentrations, the observed rate was limited by the ATP binding process; therefore, it was linearly dependent upon ATP concentration (*2*), and the slope gives an apparent second-order rate constant (K_1k_{+2}), 0.48 ± 0.09 μM^{-1} s^{-1}, for NMIIB S1. Since blebbistatin was found to be inactivated at 295 nm, the wavelength at which tryptophan fluorescence

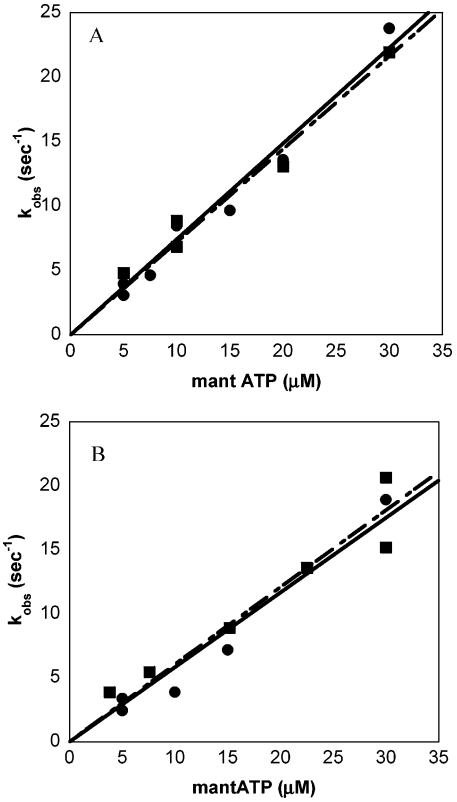

FIGURE 3: mantATP binding and hydrolysis. In panel A, 1 μM nucleotide-free NMIIB S1 with (■) and without (●) 100 μM blebbistatin was mixed with varying concentrations of mantATP in the stopped flow apparatus, and the reaction was monitored by the enhancement of mantATP fluorescence. The slope of k_{obs} as a function of mantATP concentration gave an apparent second-order rate constant (K_1k_{+2}) of 0.74 ± 0.02 μM^{-1} s^{-1} for NMIIB S1 and 0.72 ± 0.03 μM^{-1} s^{-1} for NMIIB S1 + blebbistatin. In panel B, 1 μM nucleotide-free NMIIB S1 and 2.5 μM actin with (■) and without (●) 100 μM blebbistatin was mixed with varying concentrations of mantATP in the stopped flow apparatus, and the reaction was monitored by the enhancement of mant fluorescence emission. The slope gave an apparent second-order rate constant ($K'_1k'_{+2}$) of 0.62 ± 0.04 μM^{-1} s^{-1} for NMIIB S1 and 0.56 ± 0.03 μM^{-1} s^{-1} for NMIIB S1 + blebbistatin.

is measured, the effect of blebbistatin on ATP binding could not be determined by this method.

The kinetics of ATP hydrolysis by NMIIB S1 with and without 100 μM blebbistatin treatment were measured with a chemical quench experiment. The initial burst in phosphate production observed by production of ^{32}P on mixing NMIIB S1 (with and without blebbistatin) with excess ATP indicates that hydrolysis occurs before the rate-limiting step of the process, as demonstrated in previous studies (*2*). The amplitude of the ADP−P_i burst of NMIIB S1 in the absence of actin was determined at 25 °C using activated charcoal extraction to measure $^{32}P_i$ generated from the hydrolysis of [γ-^{32}P]ATP (*11*). The mixing time before quenching was 5 s, and the final concentrations were 5 μM NMIIB S1 and 50 μM MgATP. The burst amplitude for NMIIB S1 was measured to be 0.30 ± 0.05, and blebbistatin (100 μM) treatment did not significantly change the value (0.33 ± 0.06) (Table 1). The amplitude of the initial P_i burst ([P_i]/[NMIIB S1]) can be used to calculate the equilibrium constant (P_i burst = $K_3/(1 - K_3)$) of the hydrolysis step (K_3). The calculated K_3 for NMIIB S1 was found to be 0.44 ± 0.06,

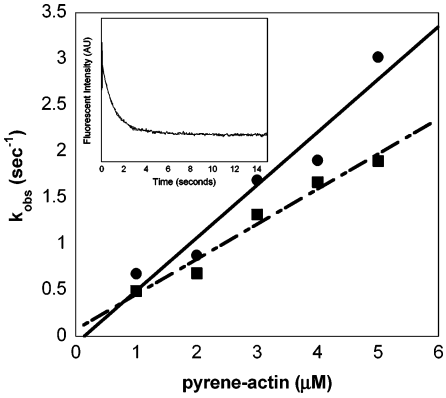

FIGURE 4: Kinetics of NMIIB S1(ADP) binding to pyrene-labeled actin filaments. NMIIB S1 was mixed with a 10-fold molar excess of pyrene-labeled actin in the presence of 0.4 μM ADP in the stopped flow apparatus. Dependence of the fast phase of the biexponential fit of k_{obs} (●) showed a rate of 0.57 ± 0.08 μM^{-1} s^{-1}, and blebbistatin (100 μM) treatment (■) showed a rate of 0.38 ± 0.03 μM^{-1}s^{-1} (inset, an averaged time course of fluorescence quenching after mixing 2 μM pyrene−actin with 0.2 μM NMIIB S1 and 0.4 mM ADP, yielding a k_{obs} of 0.9 ± 0.072 s^{-1} for the fast phase and 0.32 s^{-1} for the slow phase.)

and blebbistatin treatment of NMIIB S1 showed a K_3 of 0.50 ± 0.07.

Kinetics of NMIIB S1(ADP) Binding to Pyrene−Actin. Binding of NMIIB S1 or NMIIB S1−ADP to pyrene-labeled actin decreases pyrene fluorescence upon formation of the strongly bound actomyosin complex (Figure 4, inset). The fluorescence transient upon mixing NMIIB S1 and 0.4 mM ADP with 10-fold excess pyrene−actin was biexponential. A similar biexponential process was observed in previous studies on NMIIB S1 (1). The fast phase of k_{obs} (Figure 4) was linearly dependent on actin concentration. The slope of the fast phase as a function of actin concentration in the blebbistatin (100 μM)-treated NMIIB S1 was 0.38 ± 0.07 μM^{-1} s^{-1}, while that of untreated NMIIB S1 was 0.57 ± 0.08 μM^{-1} s^{-1} (k_{+10}). The amplitudes of the slow phase were similar (∼4% of the total amplitude) with and without blebbistatin, and the rate of the slow phase was linearly dependent on actin concentration both in the presence and absence of blebbistatin (0.07 ± 0.006 and 0.09 ± 0.01 μM^{-1} s^{-1}, respectively).

Phosphate Release. The kinetics of actin-activated phosphate release (P_i release) from NMIIB S1 was measured by sequential mixing in a stopped flow apparatus and monitoring the fluorescence of phosphate binding protein. Two micromolar nucleotide-free myosin IIB S1 was mixed with 1.5 μM ATP, the complex was allowed to age for 2 s to allow population of the myosin IIB−ADP−P_i state, and it was then mixed with 40 μM actin. Blebbistatin treatment produced a complete inhibition of P_i release (Figure 5A). This inhibition was observed for up to 1 s (Figure 5) and was followed by P_i release at a similar rate (0.05 ± 0.004 s^{-1}) and reduced amplitude to that observed in the absence of blebbistatin (0.03 ±0.003 s^{-1}) (Figure 5A, inset).

Recovery of P_i release following the 1 s inactivation period (photoinactivation of blebbistatin occurs after 1 s of exposure to 425 nm light) also showed a dose dependence on the concentration of blebbistatin. Increase in concentration of blebbistatin resulted in a reduction in the amplitude of the recovery of P_i release from NMIIB S1 after the initial

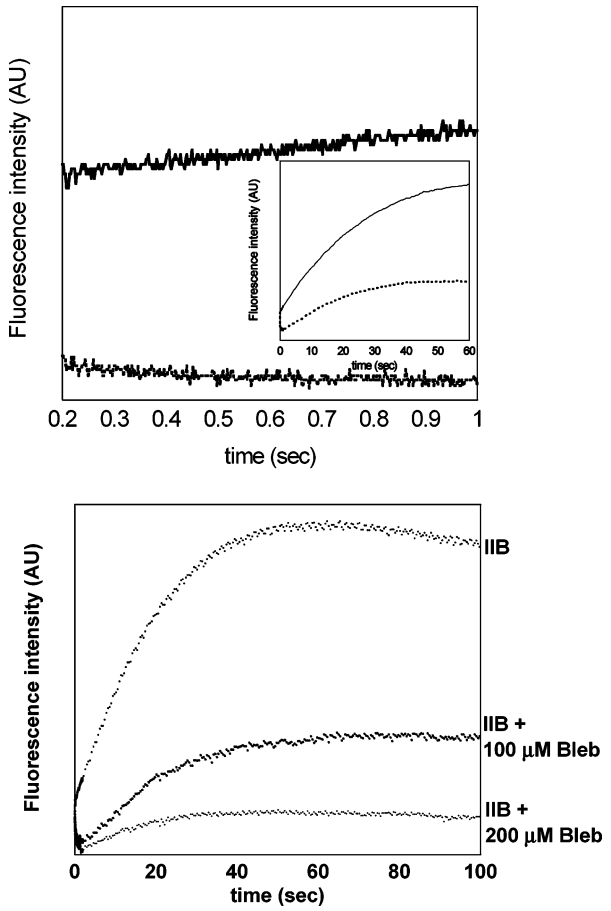

FIGURE 5: Kinetics of phosphate release. In panel A, P_i release kinetics were measured by stopped flow and monitored by the change in fluorescent emission of phosphate binding protein. The single-turnover trace shown was obtained on mixing 4 mM NMIIB S1 with (− − −) and without (—) 100 μM (±)-blebbistatin. Two micromolar NMIIB S1 in the presence and absence of blebbistatin was mixed with 1.5 μM ATP, aged for 2 s, and then mixed with 40 μM actin. The fluorescence increase was fit to a single-exponential function with k_{obs} of 0.041 s^{-1} for NMIIB S1. Blebbistatin treatment resulted in complete inhibition of P_i release until it was photoinactivated after approximately 1 s (inset, following photo inactivation of blebbistatin, a normal rate of P_i release was observed, which could be fitted to a single-exponential function with k_{obs} of 0.054 s^{-1}). In panel B, the amplitude of P_i release is dose-dependent on blebbistatin concentration. The amplitude of the recovery of P_i release by NMIIB S1, following the 1 s inhibition period, treated with 100 and 200 μM blebbistatin is reduced by 60% and 90%, respectively, compared to untreated NMIIB S1. Traces are normalized to starting values.

inhibition of signal up to 1 s, as measured by the amplitude of the fluorescence signal. Nucleotide-free NMIIB S1 (3 μM) was mixed with 2.5 μM ATP, the complex was allowed to age for 2 s, and it was then mixed with 40 μM actin (final). Compared to untreated NMIIB S1 (100%), incubation with 100 μM blebbistatin resulted in a ~60% decrease and with 200 μM blebbistatin in a ~90% decrease in the amplitude of P_i release (Figure 5B). However the rate of P_i release during recovery did not change with blebbistatin treatment. Incubation of 100 μM blebbistatin with NMIIB S1 had a recovered P_i release rate of 0.07 ± 0.004 s^{-1}, and that with 200 μM blebbistatin recovered P_i release at a rate of 0.05 ± 0.004 s^{-1} after the 1-s inhibition, while untreated NMIIB S1 showed a P_i release rate of 0.05 ± 0.0009 s^{-1}.

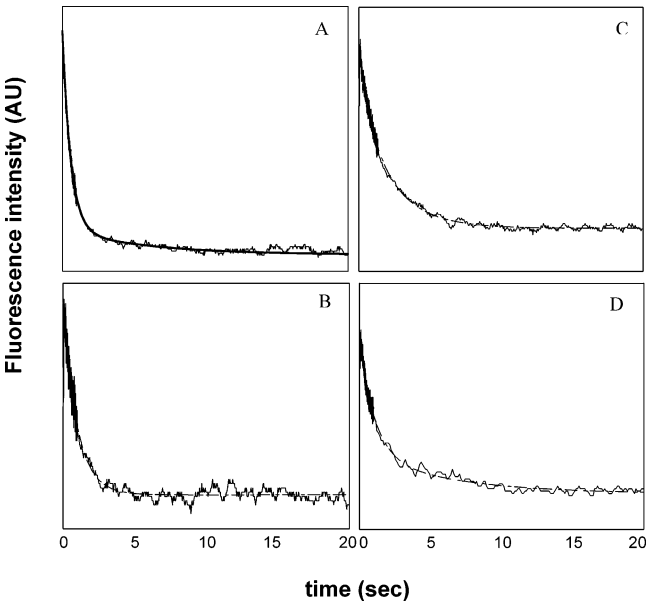

FIGURE 6: MantADP dissociation from NMIIB S1 and acto-NMIIB S1. An average time course of the mantADP fluorescence decrease as mantADP is displaced from NMIIB S1 is shown in each condition. One micromolar NMIIB S1 (A) and 1 μM NMIIB S1 + 100 μM blebbistatin (B) and 1 μM acto-NMIIB S1 (C) and 1 μM acto-NMIIB S1 + 100 μM blebbistatin (D) in the presence of 10 μM mantADP were mixed with 4 mM ATP. Although blebbistatin treatment showed a drop in the rate of ADP dissociation from NMIIB S1 and acto-NMIIB S1, DMSO had an appreciable effect on ADP dissociation. A 14% reduction in the rate of mantADP dissociation from NMIIB S1 and a 30% reduction in that from acto-NMIIB S1 normalized to DMSO effect were observed.

Dissociation of mantADP from NMIIB S1 and Acto-NMIIB S1. The dissociation of mantADP from acto-NMIIB S1 was monitored by following the mantADP fluorescence. The fluorescence signal was fitted to a biexponential curve. The initial fast rate of NMIIB S1 and acto-NMIIB S1 is inclusive of a mixed population of strong and weak ADP binding states. The subsequent slow rate is indicative of the dissociation of ADP from NMIIB S1. A decrease in fluorescence was observed upon dissociation of mantADP from NMIIB S1 (Figure 6A) or acto-NMIIB S1 (Figure 6C) after mixing with excess ATP. The observed fast rate of the decrease in fluorescence of mantADP from NMIIB S1 was 1.8 ± 0.28 s^{-1}, and that from acto-NMIIB S1 was 1.8 ± 0.22 s^{-1} (Table 1). Blebbistatin (100 μM) reduced the rate of mantADP dissociation from NMIIB S1, 1.3 ± 0.09 s^{-1} (Figure 6B), and from acto-NMIIB S1, 0.9 ± 0.1 s^{-1} (Table 1) (Figure 6D). Part of the difference observed with blebbistatin treatment was contributed by DMSO (see Table 1). DMSO treatment reduced the rate of mantADP dissociation compared to untreated controls in both NMIIB S1 and acto-NMIIB S1 (1.5 ± 0.08 and 1.4 ± 0.28 s^{-1}, respectively).

Kinetics of Binding to Actin in the Presence of ATP. We examined the rebinding of NMIIB S1 to actin following ATP-induced dissociation from pyrene−actin by performing single-turnover experiments with and without blebbistatin incubation. Dissociation from actin and rebinding in the presence of ATP was monitored by pyrene−actin fluorescence. Acto-NMIIB S1 (1 μM NMIIB S1 and 5 μM pyrene−actin) was mixed with limiting ATP (0.9 μM) in the stopped flow apparatus. In untreated NMIIB S1, following a single

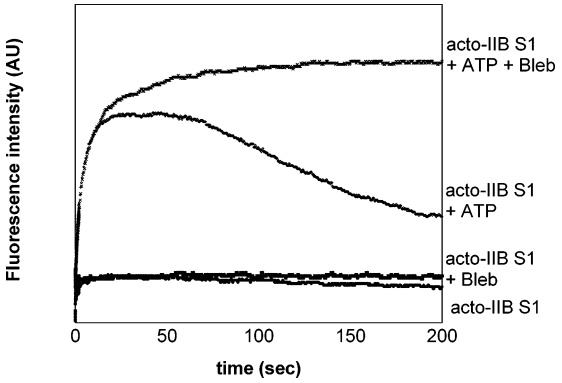

FIGURE 7: Actin rebinding in the presence of ATP. Single-turnover traces of pyrene fluorescence emission upon mixing acto-NMIIB with limiting ATP. Five micromolar pyrene−actin preincubated with 1 μM NMIIB S1 were mixed in the stopped flow apparatus with 0.9 μM ATP with and without 100 μM blebbistatin. Blebbistatin inhibits actin rebinding in the presence of ATP.

turnover the pyrene fluorescence was completely quenched as a result of rebinding to actin. Blebbistatin (100 μM) completely inhibited the rebinding of NMIIB S1 to pyrene−actin over a 100-s period, and the pyrene signal remained elevated (i.e., nonappreciable rebinding to actin was detected) (Figure 7).

DISCUSSION

Blebbistatin is a small molecule derivative of 1-phenyl-2-pyrrolidinone, which exists in two (±) enantiomeric forms. Straight et al. (*5*) have shown that the (−) enantiomer is the active form of blebbistatin and it inhibits the ATPase activity of myosin IIB. At an IC_{50} of ~2 μM, blebbistatin rapidly and reversibly blocks cell blebbing in human platelets and also disrupts directed cell migration and cytokinesis in vertebrate cells. A simple explanation of these observations is that blebbistatin affects the enzymatic cycle and in someway blocks crucial steps in the ATPase cycle of myosin IIB.

We found that blebbistatin reduces the actin-activated steady-state ATPase activity of NMIIB S1 markedly at all concentrations of actin studied. The most striking observation of blebbistatin effect on NMIIB S1 is the complete inhibition of phosphate release. This effect alone can account for the dramatic drop in ATPase activity of NMIIB S1 upon blebbistatin treatment. The affinity of the S1 for actin in the presence of ATP was also reduced perhaps because the inhibition of phosphate release prevented formation of a strongly bound actomyosin complex. Accordingly, we found in single-turnover experiments that blebbistatin prevents rebinding of S1−ADP−P_i to actin. In addition, the dissociation of ADP from acto-S1 complex was slightly reduced. However, ATP binding and hydrolysis were unaffected by blebbistatin.

Saturating amounts (50−100 μM) of (±)-blebbistatin (IC_{50} $\approx$ 2μM) were used in the experiments. Actin-activated ATPase activity of NMIIB S1 is suppressed by blebbistatin at all actin concentrations measured (0−100 μM). This is consistent with observations of suppression of the ATPase activity of fast skeletal muscle myosin by other inhibitors such as BTS (*4*) and BDM (*3*). Blebbistatin is a photosensitive compound. To test the effect of photosensitivity of the compound on ATPase activity, we exposed myosin incubated with blebbistatin to different wavelengths of light, such as 295 and 365 nm for 5 s and 425 nm for 1 s, before mixing with ATP to measure ATPase activity in an enzyme-linked NADH assay. These wavelengths are used to measure other kinetic parameters and were relevant for testing photoinactivation. This experiment showed that blebbistatin undergoes photoinactivation at two wavelengths, 295 and 425 nm. Light at 295 nm, used to measure tryptophan fluorescence changes in myosin, inactivates blebbistatin, and thereby blebbistatin does not inhibit subsequent steady-state ATPase activity. Exposure of blebbistatin-incubated NMIIB S1 to 425 nm light for 1 s shows a similar maintenance of steady-state ATPase activity. This is relevant in the context of the present study where 425 nm is used to measure P_i release, since blebbistatin is inactivated after a 1 s exposure to 425 nm light. Thus the inhibition of P_i release by blebbistatin is only seen during the first second under the assay conditions. However, 365 nm light used to monitor mant and pyrene signals does not inactivate blebbistatin.

Blebbistatin does not affect the ATP binding site, since neither ATP binding (K_1k_{+2}) nor hydrolysis ($k_{+3} + k_{-3}$) is affected (Figure 3). This observation is also similar to myosin inhibition by other inhibitors such as BTS (*4*) in fast skeletal muscle myosin. In control NMIIB S1, untreated with blebbistatin, change in tryptophan fluorescence was also used to determine ATP binding and hydrolysis. However due to inactivation of blebbistatin at 295 nm, the wavelength required to measure intrinsic tryptophan fluorescence changes, the effect of blebbistatin on ATP binding and hydrolysis could not be studied by this method. Using the initial part of the pyrene signal obtained from ATP-induced dissociation of pyrene−actin as a measure of ATP binding, a 2-fold slower binding was observed with blebbistatin (Table 1). However, using mantATP to measure ATP binding did not show a difference in binding to acto-NMIIB S1 (Figure 3). Chemical quench experiments to study the equilibrium constant of ATP hydrolysis did not show a difference in K_3 with blebbistatin (Table 1).

Fluorescently labeled phosphate binding protein was used to measure the rate of P_i release (k'_{+4}) in the presence of actin by sequential mix stopped flow experiments (Figure 5). In the stopped flow cuvette, the complex is excited by 425 nm light, and the emission is read with a 455 nm long-pass filter. Since blebbistatin is a photosensitive compound, the initial 1 s of the reaction with blebbistatin represents the true effect of the inhibitor. During this time period, a complete inhibition of P_i release is observed (Figure 5). After this, the molecule gets photoinactivated and thereby allows P_i release to proceed at the normal rate (Figure 5 inset). The dose dependence of recovery of P_i release to blebbistatin concentration is indicative of the efficacy of the molecule. A decrease in amplitude of recovery of P_i release of ~60% by 100 μM blebbistatin and ~90% by 200 μM blebbistatin was observed. This is indicative of the inactivation of a subset of NMIIB S1 population that is proportional to blebbistatin concentration. We propose that blebbistatin binds to myosin in a concentration-dependent manner and a dynamic equilibrium exists between bound and unbound blebbistatin with NMIIB S1. Further, we propose that photoinactivation of blebbistatin while bound to myosin results in a chemical modification of the myosin blocking its ability to release

phosphate. Alternatively, photoinactivation of blebbistatin may result in a reduction in its affinity for myosin, and thus higher concentrations of blebbistatin are needed to completely inhibit myosin. Thus, either one or both of these two possibilities could explain why higher concentrations of blebbistatin cause a greater inhibition of myosin following photoinactivation.

Blebbistatin decreases the rate of ADP release from the acto-NMIIB S1 (k'_{+5}) complex to a greater extent than from NMIIB S1 in the absence of actin (k_{+5}). A reduction of ~14% from NMIIB S1 and ~30% from acto-NMIIB S1 was observed. The value of k'_{+5} obtained in this study, $1.8 \pm 0.22\ s^{-1}$, is actually an apparent dissociation rate, because it has been shown that the ADP release step can be partitioned into a slow isomerization followed by a faster dissociation (*1*). (In our study, acto-NMIIB S1 complex incubated with mantADP was mixed with excess ATP to measure ADP release. To resolve the isomerization and dissociation steps, Rosenfeld et al. (*1*) mixed mantADP−NMIIB S1 with varying concentrations of actin.) Although blebbistatin reduced the rate of ADP release, DMSO also had a small effect, making it difficult to definitively quantify the contribution of blebbistatin to the decrease observed in either NMIIB S1 or acto-NMIIB S1.

Blebbistatin affects the apparent affinity of NMIIB S1 for actin dramatically in the presence of ATP and slightly in the presence of ADP. This would suggest that in both cases, the rate of the weak to strong transition on actin is being affected. Using pyrene−actin, we examined the rate of binding of NMIIB S1 to actin in the presence of ADP, which was 2-fold slower in the presence of blebbistatin. In addition, we studied the rebinding to pyrene−actin in the presence of limiting ATP. In single-turnover experiments with ATP, actin rebinding was completely inhibited. Since P_i release and actin binding are intimately linked, it is difficult to determine whether P_i release is blocked, actin binding in the ADP−P_i state is weakened, or both are affected in the presence of blebbistatin. Nevertheless, blebbistatin has a dramatic inhibitory effect on this critical stage of the ATPase cycle.

Our results, which suggest that specific steps of ATP hydrolysis are modulated by blebbistatin, may provide insight into the structural interaction of blebbistatin with S1 and acto-S1. The myosin motor domain is divided into subdomains, two of which (upper and lower 50 kD subdomains) contain the actin binding site (*13*, *14*). Structurally, these domains are divided by a large cleft that extends from the actin-binding site to the base of the nucleotide binding site (*13*). Based on structural studies, this cleft has been postulated to progressively close upon actin binding and product release (*13*, *14*) and has been observed to close in a nucleotide-free, strong actin-binding structure of myosin V (*14*). In addition, solution studies have demonstrated that the 50 kD cleft changes conformation upon binding to and dissociation from actin (*15*, *16*). Thus cleft closure is necessary for formation of the strongly bound myosin states on actin. Blebbistatin slows the rate of formation of the strongly bound actomyosin complex slightly in the presence of ADP but markedly in the presence of ADP−P_i. Thus blebbistatin likely is affecting the affinity for actin, P_i release, or both by slowing or preventing the cleft closure in myosin that allows strong binding. It may prevent closure of the cleft completely with ADP−P_i but merely slow it with ADP. These results are consistent with previous results that suggest that there is a dramatic conformational change in the cleft in the presence of ATP, while only a small change in the presence of ADP (*15*). Thus the blebbistatin binding site likely resides within the cleft, between the nucleotide pocket and actin interface. The inability of blebbistatin to inhibit other myosin isoforms (*5*) may be a result of differences in the structural dynamics of the actin-binding cleft of these different myosin isoforms. Indeed, myosin V, which has been shown to form a closed cleft conformation more readily in the absence of nucleotide (*14*), releases P_i rapidly upon association with actin (*11*). Myosin V is not inhibited by the concentrations of blebbistatin that were used in this study (*5*). Further structural studies are necessary to fully characterize the interaction between blebbistatin and myosin.

While this paper was under review, another report appeared on the effects of blebbistatin on the kinetics of skeletal muscle myosin (*17*). Their reported effects on both P_i release and ADP release agree with the values obtained in this study, as did their conclusions regarding the mode of action of blebbistatin.

REFERENCES

1. Rosenfeld, S. S., Xing, J., Chen, L. Q., and Sweeney, H. L. (2003) Myosin IIB is unconventionally conventional, *J. Biol. Chem. 278* (30), 27449−27455.
2. Wang, F., Kovacs, M., Hu, A., Limouze, J., Harvey, E. V., and Sellers, J. R. (2003) Kinetic mechanism of nonmuscle myosin IIB: functional adaptations for tension generation and maintenance, *J. Biol. Chem. 278* (30), 27439−27448.
3. Ostap, E. M. (2002) 2, 3-Butanedione monoxime (BDM) as a myosin inhibitor, *J Muscle Res. Cell Motil. 23* (4), 305−308.
4. Shaw, M. A., Ostap, E. M., and Goldman, Y. E. (2003) Mechanism of inhibition of skeletal muscle actomyosin by *N*-benzyl-*p*-toluene sulfonamide, *Biochemistry 42* (20), 6128−6135.
5. Straight, A. F., Cheung, A., Limouze, J., Chen, I., Westwood, N. J., Sellers, J. R., and Mitchison, T. J. (2003) Dissecting temporal and spatial control of cytokinesis with a myosin II Inhibitor, *Science 299* (5613), 1743−1747.
6. Duxbury, M. S., Ito, H., Benoit, E., Zinner, M. J., Ashley, S. W., and Whang, E. E. (2004) RNA interference targeting focal adhesion kinase enhances pancreatic adenocarcinoma gemcitabine chemosensitivity, *Biochem. Biophys. Res. Commun. 311* (3), 786−792.
7. Sweeney, H. L., Rosenfeld, S. S., Brown, F., Faust, L., Smith, J., Xing, J., Stein, L. A., and Sellers, J. R. (1998) Kinetic tuning of myosin via a flexible loop adjacent to the nucleotide binding pocket, *J. Biol. Chem. 273* (11), 6262−6270.
8. Pardee, J. D., and Spudich, J. A. (1982) Purification of muscle actin, *Methods Enzymol. 85* (Part B), 164−181.
9. Pollard, T. D. (1984) Purification of a high molecular weight actin filament gelation protein from Acanthamoeba that shares antigenic determinants with vertebrate spectrins, *J. Cell Biol. 99* (6), 1970−1980.
10. De La Cruz, E. M., Wells, A. L., Sweeney, H. L., and Ostap, E. M. (2000) Actin and light chain isoform dependence of myosin V kinetics, *Biochemistry 39* (46), 14196−14202.
11. De La Cruz, E. M., Wells, A. L., Rosenfeld, S. S., Ostap, E. M., and Sweeney, H. L., (1999) The kinetic mechanism of Myosin V, *Proc. Natl. Acad. Sci. U.S.A. 96*, 13726−13731.
12. White, H. D., Belknap, B., and Webb, M. R. (1997) Kinetics of nucleoside triphosphate cleavage and phosphate release steps by associated rabbit skeletal actomyosin, measured using a novel fluorescent probe for phosphate, *Biochemistry 36* (39), 11828−11836.
13. Rayment, I., Rypniewski, W. R., Schmidt-Base, K., Smith, R., Tomchick, D. R., Benning, M. M., Winkelmann, D. A., Wesenberg, G., and Holden, H. M. (1993) Three-dimensional structure

of myosin subfragment-1: a molecular motor, *Science 261*, 50−58.
14. Coureux, P. D., Wells, A. L., Menetrey, J., Yengo, C. M., Morris, C. A., Sweeney, H. L., and Houdusse, A. (2003) A structural state of the myosin V motor without bound nucleotide, *Nature 425* (6956), 419−423.
15. Yengo, C. M., De la Cruz, E. M., Chrin, L. R., Gaffney, D. P., and Berger, C. L. (2002) Actin-induced closure of the actin-binding cleft of smooth muscle myosin, *J. Biol. Chem. 277*, 24114−24119.
16. Conibear, P. B., Bagshaw, C. R., Fajer, P. G., Kovacs, M., and Malnasi-Csizmadia, A. (2003) Myosin cleft movement and its coupling to actomyosin dissociation, *Nat. Struct. Biol. 10* (10), 773−775.
17. Kovacs, M., Toth, J., Hetenyi, C., Malnasi-Csizmadia, A., and Sellers, J. R. (2004) Mechanism of blebbistatin inhibition of myosin II, *J. Biol. Chem. 279*, 35557−355563.

BI0490284